International Journal of Physics, 2018, Vol. 6, No. 3, 93-98
Available online at http://pubs.sciepub.com/ijp/6/3/5

DOI:10.12691/ijp-6-3-5

Drag Reduction by Using the Microriblet of Sawtooth and Scalloped Types

Alireza Heidarian[1], Hassan Ghassemi[2,*], Pengfei Liu[3]

[1]Department of Marine Engineering, Persian Gulf University, Boushehr, Iran
[2]Department of Maritime Engineering, Amirkabir University of Technology, Tehran, Iran
[3]Australian Maritime College, University of Tasmania, Locked bag 1395, Launceston, TAS 7250, Australia & International School of Ocean Science and Engineering, Harbin Institute of Technology, Weihai, 264200, China
*Corresponding author: gasemi@aut.ac.ir

Abstract Nowadays, considering the importance of the drag reduction and increasing the speed is demand of all owners. In the field of marine industry, there should be an ongoing attempt to reduce fuel consumption of the marine vehicles. In this research, nature has been used as a guide to reach our target. Study of the skin of the fast marine's faunas such as sharks and dolphins has generated the idea of riblet covered surfaces. Two various types of the riblets surfaces (sawtooth and scalloped) which are studied in this research. The microriblets are applied on the flat plate and investigated the effects on hydrodynamics parameters through the computational fluid dynamics method in ANSYS CFX. The results have been validated with the experimental results. By comparing the drag coefficient of simple flat plate with riblet one, it is concluded that riblets diminish drag force about 11% and raise lift about 6 % relative to the simple flat plate.

Keywords: *drag reduction, micro riblet, computational fluid dynamics, lift force*

Cite This Article: Alireza Heidarian, Hassan Ghassemi, and Pengfei Liu, "Drag Reduction by Using the Microriblet of Sawtooth and Scalloped Types." *International Journal of Physics*, vol. 6, no. 3 (2018): 93-98. doi: 10.12691/ijp-6-3-5.

1. Introduction

Nature is full of examples of structures, materials, and surfaces that can benefit science and humanity. There are several ways in nature to decrease drag force in the fluid stream, such as the evidence in the movements of fish, sharks and dolphins [1]. The phlegm covered by fish causes a decrease in drag as they pass through water, and also preserves the fish from abrasion by performing the fish slide over things rather than scrape and disease by making the surface of the fish hard for microscopic organisms to adhere [2]. Though early studies showed substantial drag reduction benefits, later studies have only been able to confirm 7% drag reduction. Defining the optimal riblet specifications for highest drag reduction is vital. Various geometries, arrangements and stuff for riblet and various fluids and flow regimes have been investigated through tests [3].

The surface of fast swimming sharks defends against biofouling and decreases the drag felt by sharks as they move through the water. The small scales covering the skin of fast-swimming sharks, identified as dermal denticles (skin teeth), are formed like small riblets and arranged in the direction of fluid flow. Riblets are useful for drag reduction of objects where the drag is caused by turbulent flow, thus proper for the long objects with fairly flat edges. Riblets are not useful on objects with pressure drag as their principal drag force [4]. Cases, where riblets were applied in practice, include the use of sawtooth riblets manufactured by 3M Company on an Olympic craft and an American sailing yacht in the mid-1980s, which proved the good effect. It was also employed on test planes, though never used on commercial flights [5]. While good results were obtained in measurement, it was calculated that only 3% drag reduction can be drawn for a commercial plane considering the limitations in the areas where riblets can be performed [6]. So far, riblets have commercially implemented in racing swimsuits specifically for drag reduction goals, which has been strongly used in Olympic by an American professional. It is stated that by wearing these swimsuits drag can be diminished by 4% for men and 3% for women [7].

The geometry of riblets includes blade, sawtooth, scalloped, and bullnose with connected and segmented configurations (aligned and staggered). A typical geometry of sawtooth and scalloped riblets is shown in Figure 1.

While something passes in a fluid, most of the drag occurs from pressure drag and friction drag. Pressure drag is made by the pressure differences between the back and front of the object, and friction drag is a consequence of both the interactions between the fluid and the object surface and attractions between the molecules of the flud [8]. The drag on an object is representative of the energy required for momentum transfer between the fluid and the object. This transfer of momentum is to produce a velocity gradient from the surface, where the velocity is zero based on the surface of the object are utilized to reduce the no-slip wall situation, to the undisturbed fluid above the surface [4].

In turbulent conditions where the fluid molecules move in nonparallel directions and thus cross flow velocities exist between the molecules, a noticeable increase in momentum transfer will occur. This increase is of high significance because any momentum transfer parallel to the object surface will increase drag.

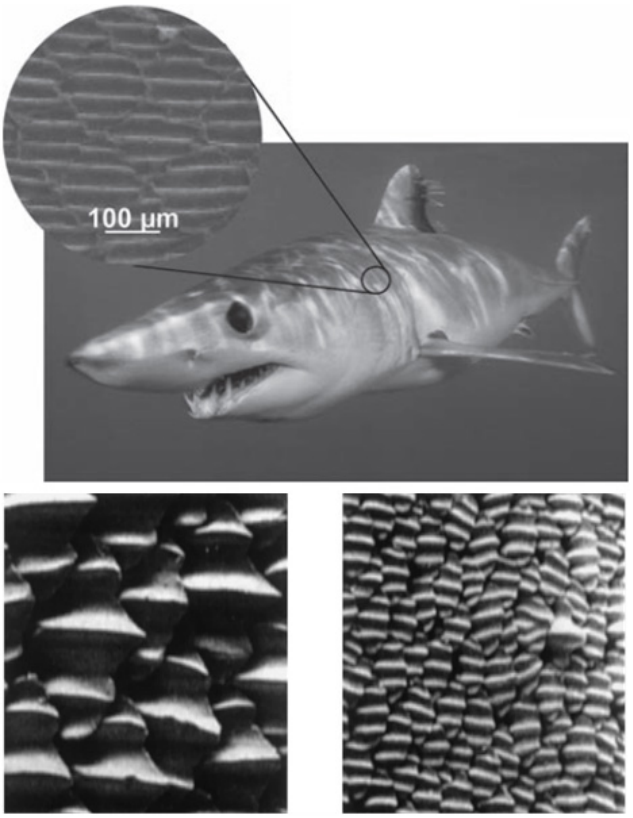

Figure 1. Different types of riblet [10]

Riblets, the small pieces covering the increased drag in turbulent flow by decreasing the momentum transfer. This is possible by the elevation of the vortices above the surface and prevention of the cross-stream movement of the stream-wise vortices in the viscous sublayer [9]. The captured image of the transition between laminar flow and turbulent flow is shown in Figure 2.

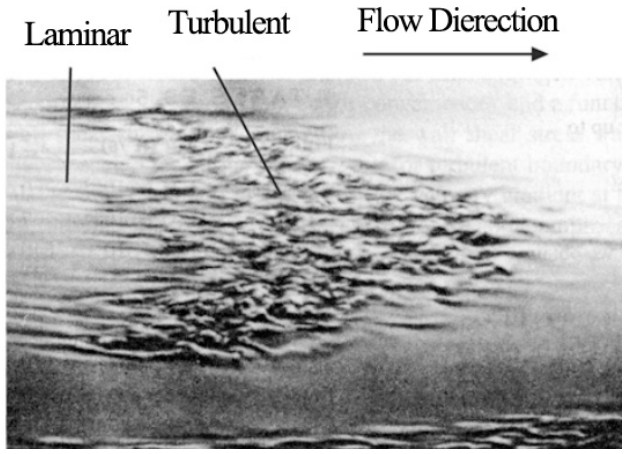

Figure 2. Transition between laminar and turbulent flow in fluid over a flat plate [9]

The use of riblet for the purpose of drag reduction does not seem obvious at the beginning, because it increases the total wetted area, thus increases the drag due to the rise in the shear stress. But, another mechanism appears here, which is the lifting of the vortices by the riblets. What happens is that riblets shift the formed vortices to around the riblet tips and fluid with lower velocity will flow between the tips [10]. Therefore, the vortices interaction is only with the small surface of the tips and high shear stress happens in this small area whereas the large area between the tips experiences a slight shear stress caused by the low velocity flow [16]. When the vortices are kept above the tips, the fluctuations of the cross stream velocity between the riblets are much lower than that above a flat plate. Therefore, the shear stress and momentum transfer is lower near a riblet covered surface, which reduces the effect of increased area due to the riblets [11].

In the present work, the physics of flow around a flat plate was investigated. The pressure distribution around the flat plate, as well as velocity around the plate were examined. This study was performed at different velocities. This work showed an in-depth investigation of flow structure around a flat plate in 2 various status of covered with riblet and without riblets which researchers and designers can eventually use the outcome as a guideline to evaluate the effects of riblets on hydrodynamics and aerodynamics parameters of.

2. Riblet Parameters

Major parameters for riblet include spacing (s), height (h), and thickness (t), which are crucial parameters to gain the best drag reduction. Figure 3 proves the geometric cross section [12]. Variations of these parameters lead to alterations in the highest drag reduction. In this research, various ratios of height to distance (h/s) for riblets were studied to choose the best type. Based on the experimental outcome of the work done by NASA and BMW on a hydrofoil boat using the riblet, the efficient kind of riblet for drag reduction is with a dimension of h/s = 0.5 for sawtooth riblets [7].

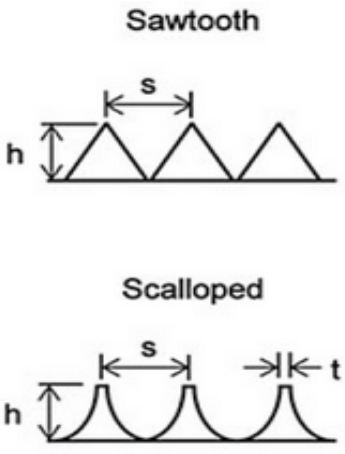

Figure 3. Geometric cross section view

To identify induced eddies and riblet structures, understanding the dimensions is required. Dimensions of the turbulent flow structures alter by the change of the flow characteristics. Hence, non-dimensional length values have been applied for better comparison of the

studies in various situations of the flow [12]. Here, all length scales were multiplied by $\frac{V_\tau}{\nu}$ and marked by plus mark (+). For instance, non-dimensional riblet spacing s^+ is given by

$$s^+ = \frac{sV_\tau}{\nu}. \quad (1)$$

Where s is the dimensional riblet spacing, ν is the kinematic viscosity, and

$$V_\tau = \left(\frac{\tau_0}{\rho}\right)^{1/2} \quad (2)$$

V_τ Represents the wall stress velocity, ρ is the fluid density and for pipe flow, the sheer stress is defined by

$$\tau_0 = 0.03955\nu^{1/4}\rho V^{7/4}D^{-1/4} \quad (3)$$

Where V is the average flow velocity and D is the hydraulic diameter, calculated for flow in rectangular pipes as

$$D = \frac{4A}{C} \quad (4)$$

Where A is the cross sectional area and C is the wetted perimeter.

Riblets performance changes with the variation of the fundamental parameters like h and s. for example, experimental data using a ratio of h/s= 0.86 showed a 9% drag reduction, while the use of h/s = 0.7 resulted in 6.5% drag reduction [5].

According to the experimental data by Bixler and Bhushan [9] the maximum drag reduction occurred in h/s=0.5 for sawtooth riblets. Based on this data, the same ratio of h/s was chosen in the present numerical simulation to observe the velocity and pressure contours and to investigate the riblets performance in reducing drag force. In the case of modeling the fluid flow, all governing equations are needed. Besides, when dealing with high Reynolds numbers, that is turbulent flow, time and space oscillations are two characteristics of the flow.

Usually, modeling these flows sounds impossible in engineering applications because oscillations happen on small scales and have high frequencies. Perhaps, in theory, these could be modeled for simple geometries and for low Reynolds numbers by using direct numerical simulation (*DNS*). Obtaining the solution of the original Navies–Stokes equations, in the case of oscillations on small scales, and high frequencies does not seem to be economically efficient at all.

3. Numerical Analysis

The Mathematical computations were done using commercial computational fluid dynamics code ANSYS CFX 16.2 [14]. The geometry is shown in Figure 4. In this simulation, a flat plate with and without riblets, in different types and dimensions of riblets was placed in the fluid flow at various velocities. There is a possibility to use five different turbulence models in ANSYS CFX including k–ε, k– ω, SST, BSL and SSG, each containing different hypotheses and equations describing the models.

RANS simulation was used in our simulations using steady-state with the shear stress transport (SST) turbulence model. The SST model applies a k–ω based model formulation in proximity of the wall and the k–ε model.

Two different types of riblets, namely sawtooth and scalloped types were used in the simulations. Scalloped riblets are most commonly defined by their h/s ratio, but test shapes have been varied between research groups. Although they are similar in their basic shapes, a standard scalloped profile has not yet been established. In general, any concave shape may be referred to scalloped. Comparison of the data from sawtooth and scalloped riblet optimizations enables a generalization of comparable shapes. The desirable tip of the riblet is thin and sharp, however good results have been produced by scalloped riblets with measurable tip thicknesses.

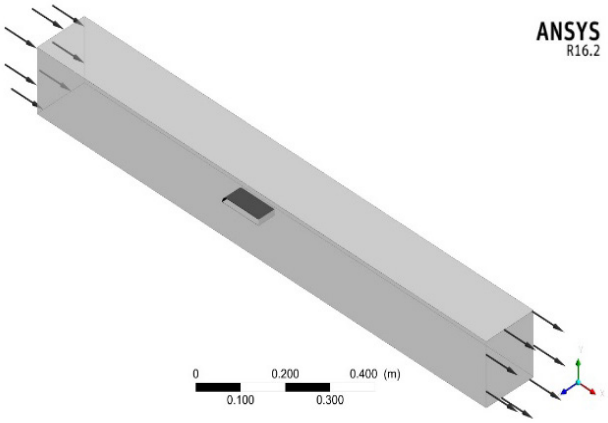

Figure 4. Flat plate in rectangular duct

3.1. Meshing

The Four different meshes representing coarse (447,401 nodes), medium (1,053,680 nodes), fine (2,238,573) and very fine (6,464,312 nodes) were examined to select the best mesh for the riblets based on the maximum y^+ and drag coefficient obtained. As it can be seen in Table 1, the drag coefficient changes from the coarse mesh to the fine mesh, where an acceptable maximum y^+=34 is achieved. This value assures that the boundary layer can be fairly well resolved on this mesh. To check the independency of the mesh, a finer mesh of 4,464,312 nodes were also examined and no variation has been obtained for the drag coefficient. Therefore, the fine mesh was selected for the simulation.

Table 1. Different meshes examined for the riblets

Mesh Type	Number of Nodes	Max y^+	Drag Coef. (C_D)
Rough	447,401	180	0.131
Medium	1,053,680	83	0.0806
Accurate	2,238,573	63	0.0179
Strict	6,464,312	34	0.0180

4. Results and Discussion

Drag reduction of different types of riblet depends on the type and dimension of riblets. For this reason, six different ratios of h/s and two types of riblets were

simulated and their drag and lift coefficients were captured based on h/s ratio and Reynolds number.

Plots in Figure 5 show numerically simulated flow over a plate without and with riblet on top of the surface. Values of drag reduction are based on the size of the riblet. The diagram represents that the drag coefficient of the riblet plate is less than a simple plate. As a result, drag force in this plate is less than a simple plate.

The largest drag reduction occurred in the ratio of about h/s=0.5 for saw-teeth riblet and about h/s=0.7 for scalloped riblets. This is the most optimal mode riblet size and the best choice for maximum drag reduction, which is also verified through experimental data. According to the chart by reducing the ratio between the height and the distance between riblets, the drag coefficient are increased. Results show optimization data for scalloped riblets. A Maximum drag reduction of 5.1% for scalloped riblets with h/s=0.7, and 11% for saw-teeth riblets with h/s= 0.5 has been obtained.

Drag reduction of various kinds of riblet depends on the type and dimension of riblets. For this reason, six different ratios of h/s and two types of riblets were simulated and their drag and lift coefficients were obtained based on h/s ratio and Reynolds number.

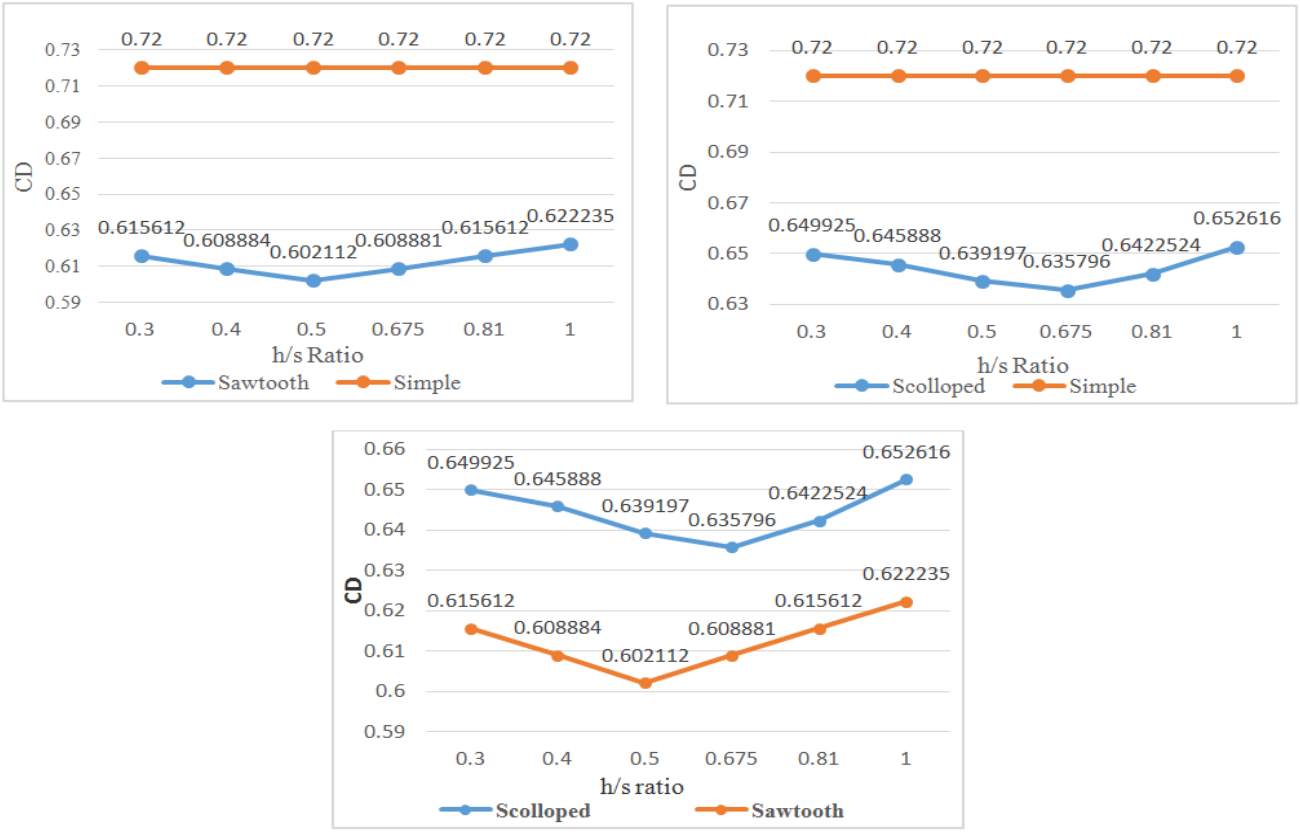

Figure 5. Comparison of various types of riblets and simple flat plate based on h/s ratio of riblets

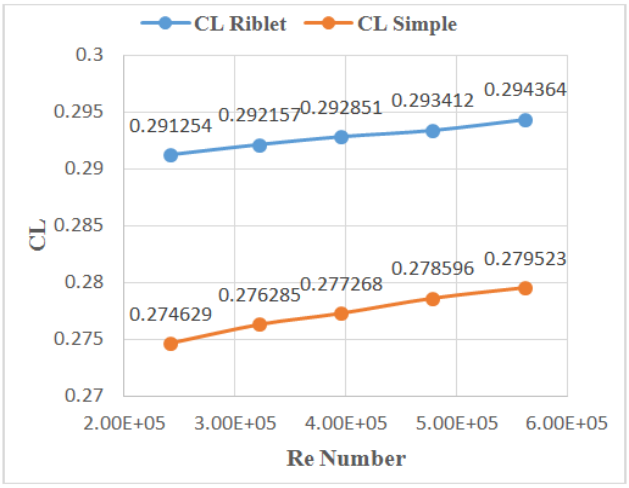

Figure 6. Lift coefficient of riblets compared with simple flat plate based Reynolds number ratio

The amount of drag coefficient for the simple flat plate was 0.72 at constant velocity has been compared to value of drag coefficient of riblet flat plate. This is the most optimal riblet size and the best option for maximum drag reduction goals, which is also validated through experimental data. According to the chart by reducing the ratio among the height and the distance between riblets, the drag coefficient is grown.

The effects of riblets on the lift coefficient have been investigated and the results are shown in Figure 6. As it can be seen from the diagrams in Figure 5 and Figure 6, increase in lift coefficient by using riblets eventually leads to the reduction in drag coefficient.

As As the sawtooth riblets had the best outcome for drag reduction purposes the lift coefficient of these riblets was compared to the simple flat plate.

The pressure contour around the riblet plate and simple flat plate are essential in drag determinations. Pressure contours obtained in $30m/s$ and two various types of riblet dimensions are represented in Figure 7. Pressure distribution in simple plate indicates that a large area of the plate is in high-value pressure meaning that the plate got higher energy.

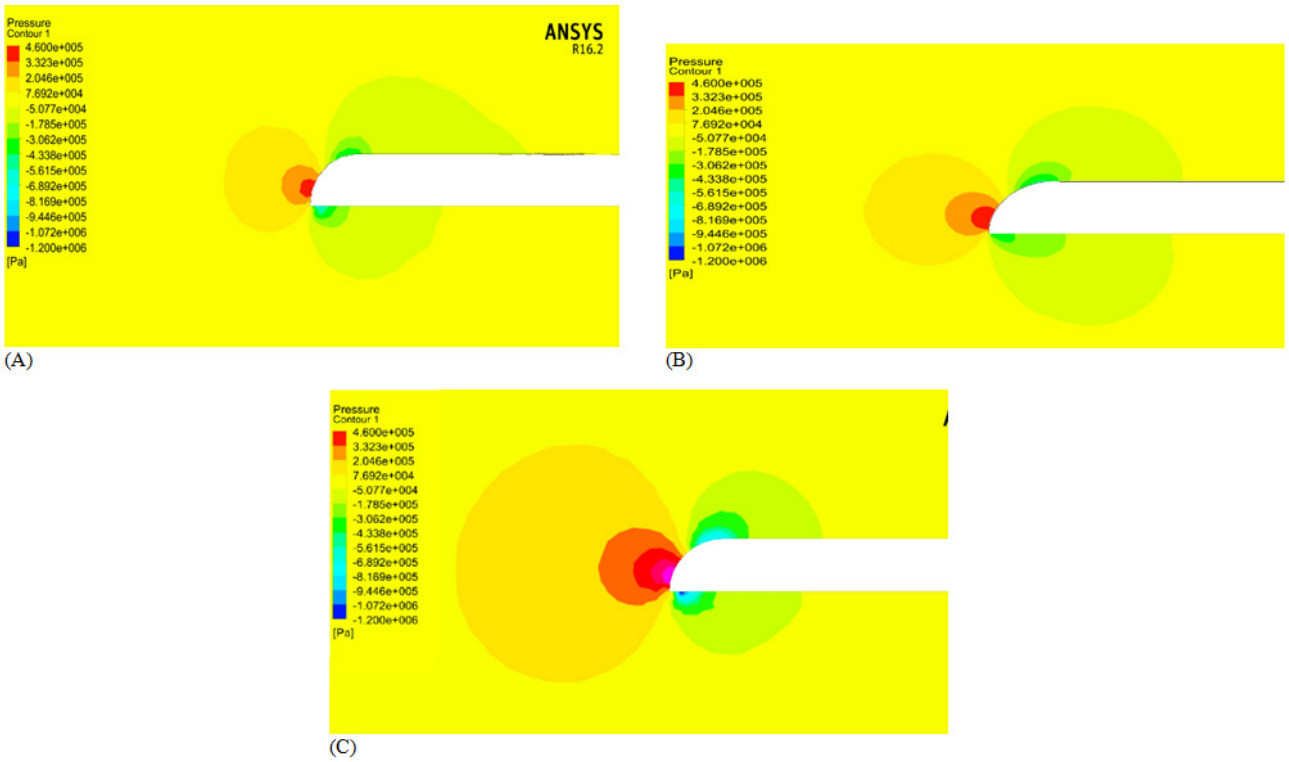

Figure 7. Pressure contour of (A): Sawtooth riblet, (B): Scalloped riblet, (C): Simple flat plate

In the flat plate with the applied riblets on surface, pressure at the tip is less than simple plate. Less pressure at the tip represents that the force of the fluid applied on the flat plate is reduced. Pressure distribution on the simple plate surface indicated that large areas of plate are in high value pressure and hence the plate receives larger force. However, pressure distribution on the simple flat plate surface is uniform and upper and lower surfaces have approximately the same pressure. As a result, lift in this type is lower than that on the riblet plate. For the sawtooth riblets with h/s=0.5 upper surface has lower pressure than the lower surface and this is the reason why this type of riblet has maximum lift compared to other types of riblet. As h/s ratios increases, the value of lift coefficient started to decrease.

Pressure distribution in riblet flat plate by h/s=162/324 shows that the pressure difference is larger than other types of riblets. More pressure gradient on the plate indicates higher lift on the flat plate. Based on the investigated results, in the simple flat plate, pressure dropped in majority parts of plate and this drop causes the separation of the fluid and increase in velocity. In scalloped riblet types, decrease of pressure at the back of flat plate is more than the sawtooth riblets.

When the pressure of flat plate is increased, it can begin to move more easily, because hydrodynamics pressure helps it to lift, thus it receives lower hydrodynamics pressure, but in other sizes of riblet, there no auxiliary force exists and it needs higher energy to move. Thus a bigger engine is needed leading to an increased cost of production. In riblet flat plate, stagnation point goes to a lower position and therefore less pressure is inserted in to sensitive areas of flat plate and pressure decreases at leading edge.

Based on the results, the separation on riblet flat plate is delayed compared to the simple flat plate. It means that major parts of flat plate have smaller pressure and force due to the reduction of fluid separation and lift force is increased in similar velocities. Bottom of riblet flat plate has smaller velocity and thus higher pressure compared to simple flat plate.

Eddy viscosity, a function of the flow, is greater for more turbulent flows. Momentum transfer by eddies in turbulent flows gives rise to an internal fluid friction. Separation on flat plates sometimes occurs around the leading edge giving rise to a short bubble. It can be dangerous because it usually occurs toward the trailing edge so the flow cannot be reattached. Therefore, the separated region merges with the wake and may cause serious structural failures.

Investigated results from numerical results from ANSYS CFX show the vortices behind a flat plate without and with riblet in different dimensions. Both types of flat plate simulated in the same condition, but final velocities in riblet types are higher than the simple flat plate. The increase in speed is due to the fluid flowing in micro-channel eliminating cross-speed component. Therefore, all the flow's energy is spent only in one direction leading to an increase in fluid turbulence.

Using microriblet film causes the flow to converge. Higher energy and momentum of the turbulent flow compared to the laminar flow can eliminate separation and the flow may reattach. A short bubble may not cause much consequence. In flight tests, total fuel consumption determines the amount of drag reduction. The 3M Corp (Minneapolis, MN) produces an experimental vinyl adhesive backed riblet sheet, which has been used in many fluid drag studies. The riblet cross sectional shape consists of equilateral triangles (sawtooth geometry) and h/s=0.516. The maximum drag reduction obtained from experiments performed by 3M riblets in different conditions together with the results of the present simulation are given in Table 2.

Table 2. Maximum drag reduction of different types of riblet in different fluids from experiments and present study

Fluid	Riblet Design	Drag Reduction	Ref.
Water	Sawtooth	6%	[1]
Water	Sawtooth	9%	[15]
Water	Sawtooth	13%	[3]
Oil	Blade Riblet	9.9%	[6]
Air	Sawtooth	8%	[2]
Air	Sawtooth	8%	[1]
Water	Sawtooth	11%	Present study

The results of series of simulations with ANSYS CFX were completely checked with the given results of former experiments. The modeled riblets were as the same size as the ones which were utilized in practice, and a good agreement were found.

5. Conclusions

This research is numerically investigated the effects of the riblets on hydrodynamics parameters of submerged flat plate in water fluid, with respect to two types of riblets, with different h/s ratios and Reynolds numbers. In this investigation, different types of microriblet include sawtooth and scalloped riblet have been simulated using ANSYS CFX software. Results reveal that skin friction drag is efficiently reduced by the use of riblets through lifting turbulent vortices. Effects of transverse shear stress and momentum transfer is minimized by vortices lifting. Experimental data performed with the riblets of 3M Company were compared with the present numerical results. By comparing the drag coefficient of simple flat with riblet one, it is concluded that riblets reduce drag force about 11% and increase lift production of about 6% of that of simple flat plate. Finally, it was shown that sawtooth riblet is the better than the scalloped one for drag reduction purposes.

Acknowledgements

The numerical computations presented in this paper have been performed on the parallel machines of the High Performance Computing Research Center (HPCRC) at Amirkabir University of Technology (AUT), their support is gratefully acknowledged. The authors received no direct funding for this research.

References

[1] Walsh M., Lindemann A, Optimization and application of riblets for turbulent drag reduction, in 22nd Aerospace Sciences Meeting. 1984, American Institute of Aeronautics and Astronautics.

[2] Davies, C. and Carpenter P.W., Numerical simulation of the evolution of Tollmien-Schlichting waves over finite compliant panels. Journal of Fluid Mechanics, 1997. 335: p361-392.

[3] Bechert, W.D., M. Bruse, and W. Hage, Experiments with three-dimensional riblets as an idealized model of shark skin. Experiments in Fluids, 2000. 28(5): p. 403-412.

[4] Dean, B. and B. Bhushan, Shark-skin surfaces for fluid-drag reduction in turbulent flow: a review. Philosophical Transactions of the Royal Society A: Mathematical, Physical and Engineering Sciences, 2010. 368(1929): p4775.

[5] Bhushan, B., Shark skin Surface for Fluid-Drag Reduction in Turbulent Flow, in Biomimetics: Bioinspired Hierarchical-Structured Surfaces for Green Science and Technology, B. Bhushan, Editor. 2012, Springer Berlin Heidelberg: Berlin, Heidelberg. p. 227-265.

[6] Bechert, D., et al., Biological surfaces and their technological application - Laboratory and flight experiments on drag reduction and separation control, in 28th Fluid Dynamics Conference. 1997, American Institute of Aeronautics and Astronautics.

[7] Krieger, K., Do Pool Sharks Swim Faster? Science, 2004. 305(5684): p. 636-637.

[8] Fuaad, P.A., M.F. Baig, and H. Ahmad, Drag-reduction in buoyant and neutrally-buoyant turbulent flows over super-hydrophobic surfaces in transverse orientation. International Journal of Heat and Mass Transfer, 2016. 93: p. 1020-1033.

[9] Bixler, G.D. and B. Bhushan, Biofouling: lessons from nature. Philosophical Transactions of the Royal Society of London A: Mathematical, Physical and Engineering Sciences, 2012. 370(1967): p. 2381-2417.

[10] Heidarian, A., Ghassemi, H., & Liu, P., Numerical Analysis of the Effects of Riblets on Drag Reduction of a Flat Plate, Journal of Applied Fluid Mechanics, 2018, 11(3), 679-688.

[11] Goldstein, D., R. Handler, and L. Sirovich, Direct numerical simulation of turbulent flow over a modeled riblet covered surface. Journal of Fluid Mechanics, 1995. 302, p333-376.

[12] Bhushan B., Biomimetics: Bioinspired Hierarchical-Structured Surfaces for Green Science, 2nd Editor, Springer publication, 2016.

[13] Bechert, D.W., et al., Experiments on drag-reducing surfaces and their optimization with an adjustable geometry. Journal of Fluid Mechanics, 1997, 338: p. 59-87.

[14] ANSYS CFX-Solver Theory Guide. 2015.

[15] Shephard, K.L., Functions for fish mucus. Reviews in Fish Biology and Fisheries, 1994. 4(4): p. 401-429.

[16] Heidarian A., Ghassemi H., Liu P., Numerical Aerodynamic of the Rectangular Wing Concerning to Ground Effect. American Journal of Mechanical Engineering, 2018, Vol. 6, No. 2, 43-47.